# DYNAMIC CHARACTERISTICS OF NICKEL TITANIUM SHAPE MEMORY ALLOY AS A CONSTRUCTION MATERIAL

by

Toshibumi Fukuta[1] and Yoshikazu Kitagawa[2]

## ABSTRACT

The tensile characteristics of shape memory alloy (SMA) wire of diameter 1 - 2 mm have been documented in studies of parameters such as the stress-strain relationship, temperature change, and strain velocity under super-elastic conditions. In order to be used in construction, SMA needs to be suitably strong and rigid. Few studies to date have examined the dynamic characteristics of SMA materials with large cross-sectional area. The experiments reported here were designed to clarify the stress-strain relationship in SMA bars in super-elastic alloy phase under compressive and tensile forces. The results are discussed below in relation to relevant parameters such as strain rate.

**KEY WORDS**: shape memory alloy
super-elasticity
stress-strain relationship
compression/tension
static load
dynamic load

## 1. INTRODUCTION

Shape memory alloy (SMA) is a unique material that, when subject to stress, exhibits a "memory shape" effect linked to temperature and also undergoes changes in basic properties such as super-elasticity[1]. These characteristics could potentially be applied to buildings to allow a degree of control over the building's behavior in response to external forces, opening up new possibilities in building design. Although the tensile characteristics of thin wire have already been reported in experiments on the stress-strain relationship, temperature change, and strain rate under super-elastic conditions[2], little is known about how SMA behaves when subjected to stress. This study was designed to determine experimentally the stress-strain relationship in SMA bars in super-elastic alloy phase when subjected to compressive and tensile forces. The results are presented below.

## 2. COMPOSITION OF TEST SPECIMEN

The alloy composition and manufacturing conditions were carefully selected so that the experimental specimen would exhibit super-elastic properties at room temperature. The exact composition was Ni 54.51%, Co 1.48%, and the remainder Ti. Table 2 shows transformation temperatures as measured using a differential scanning calorimeter.

## 3. METHODOLOGY

The specimen was a 16 mm length of bar of diameter 7 mm, which was fabricated from a parallel section of a longer length of bar of diameter 17 mm

[1] Director of IISEE, Building Research Institute, Tachihara 1, Tsukuba, Ibaraki, 305-0802, Japan, Dr. Eng.
[2] Professor, Keiou-Gijuku University, Kouhoku-ku, Hiyoshi 3-14-1, Yokohama, Kanagawa, 145-8522, Japan, Dr. Eng.

Table 1 Transformation temperature

| transformation temperature | Martensitic transformation start temperature | Martensitic transformation end temperature | Reversible transformation start temperature | Reversible transformation end temperature |
|---|---|---|---|---|
| centigrade | 25.5 | -19.0 | 8.9 | 43.2 |

(see Figure 1). The top and bottom ends were clamped in hydraulic chucks with the centres perfectly aligned. Axial forces were then applied. (Hereunder, "specimen" refers to the parallel piece of 7-mm diameter bar.) To measure the strain on and temperature of the specimen, two strain gauges, one of which also doubled as a thermocouple, were affixed on either side of the center of the parallel section, and an 8 mm extensometer was attached across the gauges.

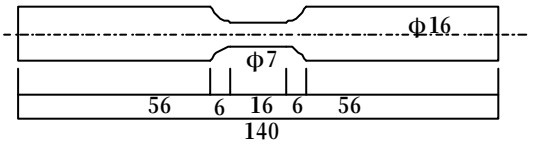


Fig. 1 Test Specimen

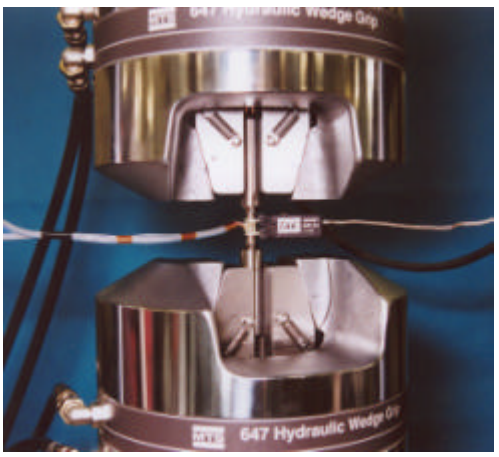

Photo 1 Test Set Up

Picture 1 shows the specimen set up in the experimental apparatus. The ambient temperature was around 26° C during the experiment. The readings from the two facing strain gauges were monitored to see whether the test piece was centrally loaded. The readings deviated from one another only very slightly during the experiment. Similarly, eccentricity under the compression load did not reach significant levels. Both static and dynamic loads were applied to the specimen by controlling the distance between the chucks with respect to displacement and velocity. The load waveform used a triangular displacement-time relationship for both static and dynamic loads.

## 4. RESULTS AND DISCUSSION

### 1) Static tensile test

Figure 2 shows the stress-strain relationship for the static tensile test. The experiment began with three repetitions at each level (0%–1%, 0% – 2%, etc.), as shown by the solid line. The specimen was then placed in a hot water bath at 50° C (hotter than the temperature at the end of the reverse transformation) for ten minutes, and repetitions were performed during unloading (at 0% – 2%, 2% – 4%, etc.). The strain generally returned to zero after each loading, clearly indicating super-elastic properties. Strain hardening can be observed from around 4% strain, where the curve gradient starts increasing. A very small amount of residual strain was observed after

removal of the strain (approximately 4.5%).

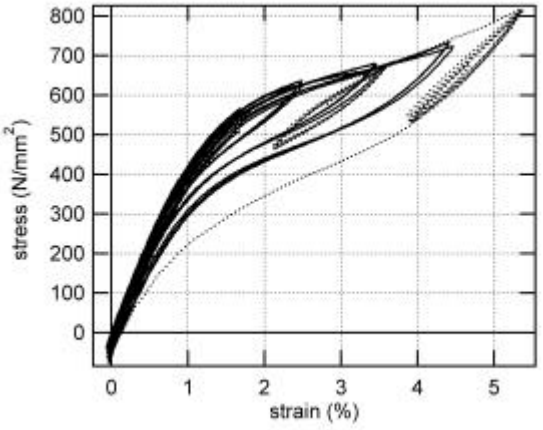


Fig.2 Stress-Strain Relationship for Static Tension Test

**2) Static compressive test**

As Figure 3 shows, the experiment was conducted in two stages. The first stage consisted of three repetitions at each of the target strain values: 0% – 1%, 0% – 2%, 0% – 3%, 0% – 4%, and 0% – 5% (actually closer to 6%). The specimen was then placed in hot water (50° C) for ten minutes, and three repetitions were performed at each of the following target strain values: 0% – 2%, 2% – 4%, and 4% – 6%. Since the load was controlled by the distance between the two chucks, the paths or trajectories the stress-strain curve took were not exactly the same for all the sets of tests, because of the residual strain that remained in the test piece after removal of the load.

Figure 3 shows the results of both the first half of the experiment (solid line) and the second half (broken line), with the second half results shifted in parallel with the strain axis at the conclusion of the first half. The stress-strain curve for compression forces differs in shape from the tension curve in Figure 2. The strain value shows no sign of the super-elasticity which would cause it to revert to zero upon removal of the load. The residual strain in fact resembles the stress-strain relationship for cold-worked carbon steel.

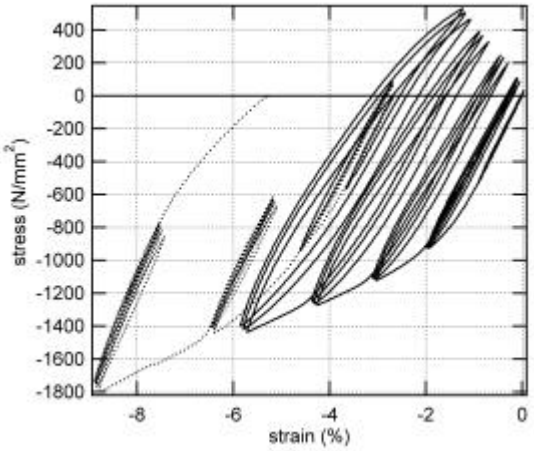


Fig.3 Stress-Strain Relationship for Static Compression Test

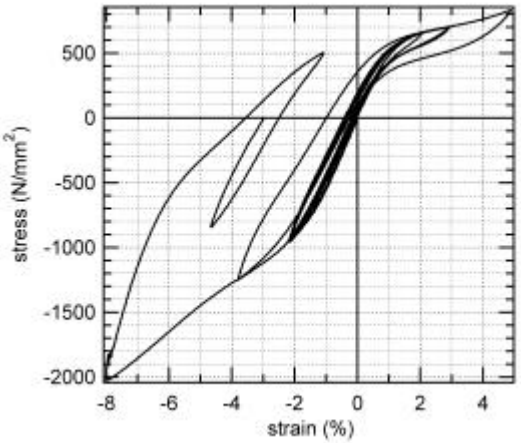


Fig.4 Stress-Strain Relationship for Static Compression-Tension

**3) Static tensile-compressive test**

Figures 4 and 5 show the results of the tensile-compressive tests. The stress-strain relationship differs in many respects (yield strength, rigidity of plateau area after yielding, final strain value after removal of load) between the tension and the compression tests. The load amplitude was approximately 4% for both compression and tension tests. Residual strain was observed after compression, but this could be negated

almost completely by then applying a tensile strain that was greater (in absolute terms) than the compression strain that caused the residue.

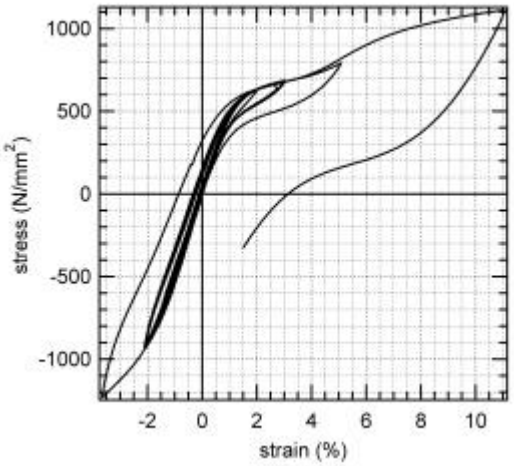


Fig.5 Stress-Strain Relationship for Static Tension- Compression

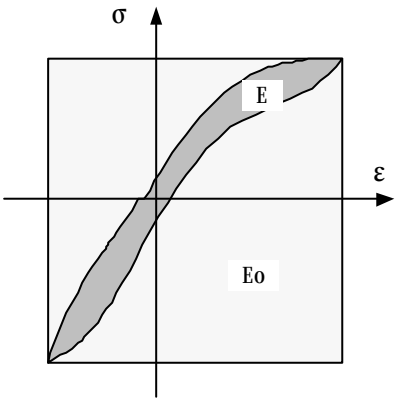


E : area covered by a stress-strain curve
Eo : area of circumscribing rectangle
E/Eo : ratio of energy absorption

Fig.6 Definition for E/Eo

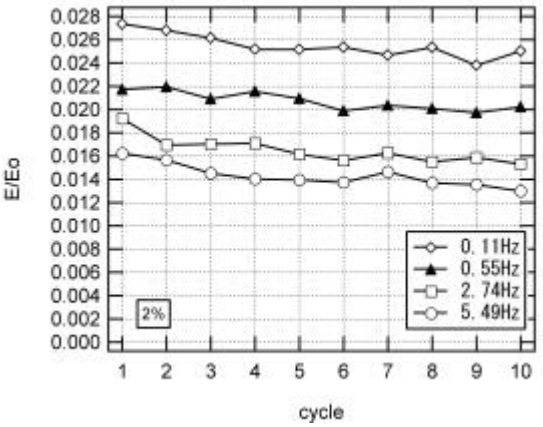


Fig.7 E/Eo for 2% Amplitude of Strain

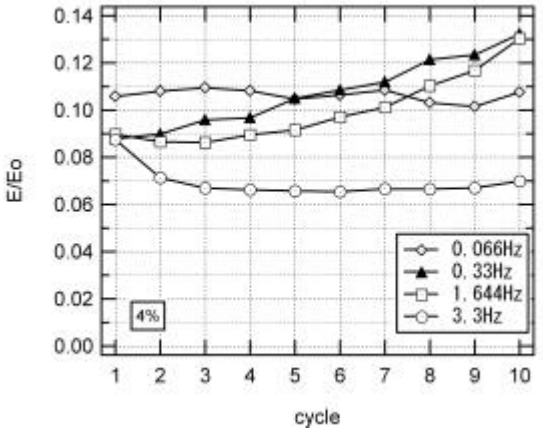


Fig.8 E/Eo for 4% Amplitude of Strain

**4) Dynamic tensile-compressive test**

The load waveform was triangular. The amplitude was varied at ±1%, ±2%, and ±4%, in that order. Four different loading frequencies (0.066 Hz, 0.33 Hz, 1.64 Hz, and 3.3 Hz) were used at each amplitude. Ten repetitions were performed for each set of conditions. Figures 7 and 8 represent the repetition loop area E shown in Figure 6 divided by the area Eo of the rectangle inscribed by the loop, for 2% and 4% amplitude, respectively. Energy absorption per cycle was determined by comparing the loop area for a single cycle with the area of the rectangle that circumscribes the loop, as described above. (The equivalent attenuation method cannot be applied directly in this situation due to

differences in the load-carrying capacity at peak times between the tension and compression sides in the stress-strain curve for SMA.) The energy absorption rate per cycle differs according to the strain amplitude: at 2% strain amplitude, the higher strain velocity causes the energy absorption rate to decrease, while at 4% strain amplitude, there was no simple correlation between the strain velocity and the rate of energy absorption.

## 5. CONCLUSIONS

This study looked at the stress-strain relationship for a columned specimen of diameter 7 mm taken from a bar of diameter 17 mm. The experiment was conducted with the specimen at the super-elastic alloy phase temperature. The specimen was subjected to static and dynamic compressive and tensile stress. The test results demonstrated that the stress-strain curve for tensile stress is completely different from that for compressive stress, irrespective of whether the load is static or dynamic in nature. This can be attributed to the differences in: initial elasticity and rigidity; yield strength and strain; yield plateau rigidity; strain path during removal of load; and residual strain. Super-elasticity was clearly evident under tensile strain of up to around 5%, but not under compressive strain, due to the presence of residual strain.

## ACKNOWLEDGMENTS

This study was carried out by the Effector Section (led by University of Tokyo professor Takashi Fujita) of the Super-Intelligent Construction Systems Development project (headed by University of Tokyo professor Shunsuke Otani), a joint research project between Japan and the United States. The authors wish to convey their thanks to all involved.

## REFERENCES

1) T. Funakubo and et al., “Shape Memory Alloy”, Sangyotosho, June 1984

2) Hiroyuki Tamai and Yoshikazu Kitagawa, ”Pseud elastic behaviour of shape memory alloy wire and its application to seismic resistance member for building”, IWCMM10, Aug., 2000, Galway, Ireland